Decoding of Intentional Actions from Scalp Electroencephalography (EEG) in Freely-behaving Infants

Zachery R. Hernandez, Jesus Cruz-Garza, Teresa Tse and Jose L. Contreras-Vidal – *IEEE Senior Member*

***Abstract*—The mirror neuron system (MNS) in humans is thought to enable an individual's understanding of the meaning of actions performed by others and the potential imitation and learning of those actions. In humans, electroencephalographic (EEG) changes in sensorimotor α-band at central electrodes, which desynchronizes both during execution and observation of goal-directed actions (i.e., μ suppression), have been considered an analog to MNS function. However, methodological and developmental issues, as well as the nature of generalized μ suppression to imagined, observed, and performed actions, have yet to provide a mechanistic relationship between EEG μ-rhythm and MNS function, and the extent to which EEG can be used to infer intent during MNS tasks remains unknown. In this study we present a novel methodology using active EEG and inertial sensors to record brain activity and behavioral actions from *freely-behaving* infants during exploration, imitation, attentive rest, pointing, reaching and grasping, and interaction with an actor. We used δ-band (1-4Hz) EEG as input to a dimensionality reduction algorithm (locality-preserving Fisher's discriminant analysis, LFDA) followed by a neural classifier (Gaussian mixture models, GMMs) to decode the each MNS task performed by freely-behaving 6-24 month old infants during interaction with an adult actor. Here, we present results from a 20-month male infant to illustrate our approach and show the feasibility of EEG-based classification of freely occurring MNS behaviors displayed by an infant. These results, which provide an alternative to the μ-rhythm theory of MNS function, indicate the informative nature of EEG in relation to intentionality (goal) for MNS tasks which may support action-understanding and thus bear implications for advancing the understanding of MNS function.**

I. Introduction

The discovery of mirror neurons in area F5 of the macaque monkey brain by Rizzolatti and colleagues [1] is considered one of the most influential neuroscience discoveries by challenging the notion of segregate sensory and motor functions in the brain. This suggested that action observation and action performance, by sharing the same neural network substrates, enabled individuals to understand other's people actions and experiences. In humans, the hypothesized MNS system has been studied extensively using scalp EEG. These studies have used changes in sensorimotor α-rhythms, also known as the μ-rhythm, to be a primary electrophysiological marker of MNS function in human infants and adults [2]. Unfortunately, several developmental (e.g., how these infants come to understand and acquire their first actions and the paucity of MNS data in infants) [3], [4] methodological [2], [5], and interpretive [6] issues need to be addressed to advance our understanding of human mirror neuron function.

Moreover, while studies are necessarily targeted to address specific questions in highly controlled lab environments, it is increasingly recognized that the processes being measured clearly do not occur in isolation and that these environments do not represent the daily behaviors of these infants at home or at play. Virtually all experimental studies in humans involve multiple cognitive components. Movement, language and memory underlie much of our existence. Subjects performing an experimental task must understand the task instructions, store them in memory, and retrieve them at the appropriate times. These processes, in turn, require executive control. Finally, competing intentions must be prioritized, sequenced, and translated into motor output, whether in the form of speech or movements. Such actions are often benefitted from extended practice and are formed and refined during development. Indeed, developmental considerations often blur these components, and thus they add to the problem. Thus, it is unclear how the above processes are accomplished in the developing infant brain. To address some of these issues, we have developed a novel experimental methodology to test freely-behaving infants while acquiring accurate information about brain activity and movement thru non-invasive means. We then deploy advanced machine learning methods to infer behavioral state or intent via scalp EEG.

The classification and prediction of movement intent using invasive ECoG and non-invasive EEG methods has long been studied, usually in research related to the fields of brain-computer interfaces and neuroprosthetics [7], [8]. However, such studies generally focus on the prediction of the kinematics of functional movements; the prediction of emotional, expressive, and contextual properties of movements has not been as well studied [8], even though such properties can affect the kinematics of a motion [9]. To the best of our knowledge, although the neural basis of the action-intention has been studied, especially during changes in μ–rhythm [10], little is known of this basis in infants. This gap in our knowledge raises many questions that could be addressed in future studies, such as how kinematics and neural activity could be used to uncover the mechanisms

Z.R. Hernandez (corresponding author, zrhernandez@uh.edu; phone: 713-743-0796; fax: 713-743-4444), T. Tse (twtse@uh.edu), and J.L. Contreras-Vidal (JLContreras-Vidal@uh.edu) are with the Non-Invasive Brain-Machine Interface Systems Laboratory at the Department of Electrical and Computer Engineering, University of Houston (UH), Houston, TX, 77004, USA.

J.G. Cruz-Garza is with the Center for Robotics and Intelligent Systems, Tecnologico de Monterrey, Monterrey Mexico.

Research supported by NIH NICHD Award PO1HD064653. We acknowledge the assistance of Yu Zhang, Michelle Edwards, Saveem Afraz, Hiba Qadri and Kathleen Bryan in the data acquisition.

behind movement intention and motor planning as well as the complexity of the intention (e.g. emotion, purpose, etc.) of the developing brain of an infant [11]. Before answering these questions, however, we must first demonstrate the feasibility of using high-density scalp EEG to decode goal-oriented movement intentions in freely-behaving infants.

In this case study, we analyzed a 15-minute session of the interactions between the infant subject and the experimenter or actor. We then segmented the infant's actions into 6 classes: wakeful attentive rest, pointing, reach-to-grasp, reach-to-give, and manipulating an object to either explore its characteristics or to imitate an action performed by the experimenter. We first conducted an exploratory analysis of both neural and motion activity data to examine any evidence of motion artifacts. Classification of movements were further conducted using a two-step machine learning algorithm that reduces the dimensionality of our feature space of EEG data while preserving local features and then generating statistical models to fit and validate the success rate of classifying movement intentions of the infant.

II. Methods

A. Experimental Design and Data Acquisition

Seven healthy infants (four female, three male) were recruited and given informed consent by their parent(s) or guardian as subjects for this study. Each infant's age ranged from 6 to 24 months. Here, we focus on the analysis of a 20-month male infant. Multiple streams of data were acquired synchronously during the experiment. Neural activity was recorded using a 64-channel, active electrode EEG scalp cap sampled at 1000 Hz (BrainAmpDC with actiCAP, Brain Products, GmbH). The electrode sets were labeled according to the 10-20 international electrode montage system with FCz and AFz labeled as reference and ground, respectively. Motion was captured using four inertial measurement units (IMUs) sampled at 128 Hz (OPAL, APDM Inc., Portland, OR) attached to the head, trunk, and arms of the subject. Gravity-compensated (GC) triaxial acceleration data was estimated by applying a Kalman filter to predict IMU orientation within a global frame and removing the effects of acceleration due to gravity [12]. In order to conduct a visual inspection of the experiment and select behavioral actions of interest, we recorded the experiment with a video camera (SDR-H100, Panasonic Co.).

The subject was seated in front of the experimenter/actor with a small table. Throughout the testing session, the experimenter gave to the subject a series of 14 toys and various objects to interact and play with at random sequence. The experimenter would also interact with the toys and show the subject how to play with some of the toys (e.g. winding up a wind-up toy). After testing, the video was visually inspected and the subject's behavioral actions were divided into six classes (shown as task {number of trials, number of samples}) described below and depicted in Fig. 1:

Attentive Rest {17 trials, 7595 samples}: A neutral state of wakeful attentive observation containing minimal to no movement.

Point {10 trials, 922 samples}: The use of the index finger to avert the other person's (in this case, the experimenter) gaze.

Reach-Grasp {34 trials, 9077 samples}: Producing a reaching motion in order to grasp the object (toy).

Reach-Offer {24 trials, 2740 samples}: Producing a reaching motion in order to offer back the object (toy) to the experimenter.

Explore {31 trials, 16552 samples}: A brief interaction with the held object to examine its features and is usually performed instead of 'Imitate'.

Imitate {15 trials, 1966 samples}: The successful imitation of the experimenter's maneuver of the object.

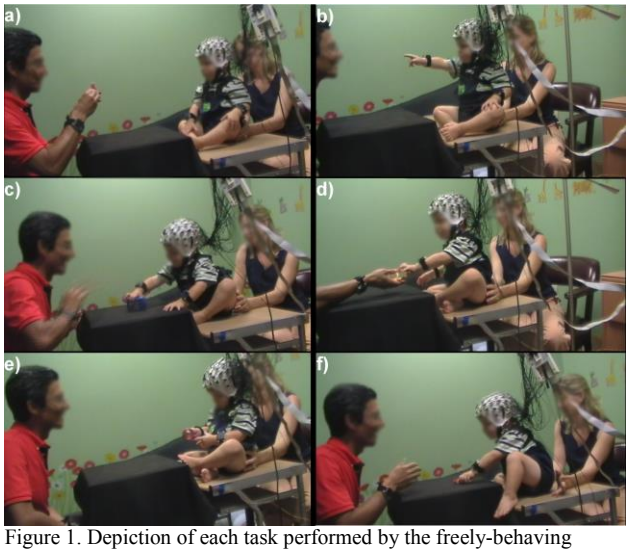

Figure 1. Depiction of each task performed by the freely-behaving infant. *Task-based classes shown are: a) Attentive Rest, b) Point, c) Reach-Grasp, d) Reach-Offer, e) Explore, and f) Imitate.*

B. Pre-processing of EEG

EEG and GC-magnitude acceleration from the entire session were truncated using the start and end-session triggers synchronized to all data streams, including the video recording. Start and end time points were recorded for various trials of each task throughout the video and used to develop a target class time vector for classification analysis as illustrated in Fig. 2. The number of time samples for all classes constituted 42.25% of the total time of the truncated session. EEG electrodes, or channels, with high impedance (defined as the frequency-dependent opposition to alternating current flow at the scalp-electrode interface) values (AF7, Cz, C2, C3, C5, CP4, P2, P6, P8, PO3-4, PO7-8) [$Z > 60$ kΩ] and peripheral channels (FP1-2, AF7-8, F7-8, FT7-10, T7-8, TP7-10, P7-8, PO7-8, O1-2, Oz, PO9-10) were rejected from the electrode set, leaving us with 32 channels to use for further analysis. Both EEG and acceleration were then resampled to 100 Hz and compared by computing a spectrogram and short-time coherence of selected channels of data to examine any effects of motion artifacts possibly affecting the EEG signal.

Before decoding, EEG signals were then band-pass filtered within the delta frequency band (1 – 4 Hz) using a 3rd order, zero-phase Butterworth filter. A lag-based feature matrix was then constructed by selecting an initial time point *(t1)* at 100 milliseconds leading the actual start time *($t_0 = t_1$ - 100)* of the signal and decremented every 10 milliseconds *(t_1, t_1-90, t_1-80, t_1-70,..., t_0)* thus resulting in 10 lags per channel. All lags per channel were concatenated and standardized by feature to form our feature matrix for the classifier.

C. Cross Validation

To reduce bias and to minimize the potential effects of artifacts, time sample data of each class were selected separately at random for training and testing the classifier. Given the variation of samples size per class, the training set size was chosen to be a percentage of the smallest class sample size. 50% of this sample size was used for training and the remaining 50% for testing. All randomly selected samples were selected either for training or testing the classifier, hence no overlapped samples.

D. Classification Algorithm

The Local Fisher's Discriminant Analysis-Gaussian Mixture Modeling (LFDA-GMM) algorithm has been employed in multiple studies [8], [13] and shown to be a robust and proficient tool for reducing the dimensionality of the lagged-based EEG feature space into a classifiable multimodal subspace in both offline and online analyses. It operates by first executing LFDA and computing a transformation matrix to limit the number of features to a reduced set of dimensions by minimizing the variance of samples within-class and maximizing the variance between classes while maintaining the each class sample's locality. Mathematical derivations proving and testing this method are further explained in studies by Sugiyama [14].

Classification of each task was conducted by fitting a distribution of random training samples into a cumulative model of one or more Gaussian distributions, each with its own factoring weights (α_k), covariance (Σ_k), and means (μ_k), as governed by the probability density function (pdf)

$$p(x) = \Sigma_{k=1\ldots K} (\alpha_k \phi_k), \quad (1)$$

where the function ϕ_k is defined as

$$\phi_k(x) = \exp\{-0.5(x-\mu_k)^T \Sigma_k^{-1}(x-\mu_k)\}]/[(2\pi)^{d/2}|\Sigma_k|^{1/2}]. \quad (2)$$

An estimation-maximization (EM) algorithm was then employed to converge upon the set for each of the three pdf (1), (2) parameters and Bayes Information Criterion (BIC) used to determine the optimal set of K Gaussian distributions for a particular class [13]. Posterior probabilities were calculated for each test sample based on the class-defined GMM such that any given sample could contain likelihood to fall within a particular class. The maximum posterior probability was chosen per test sample to discretize each class and compute classification accuracy rates. Additional information can be provided here [8].

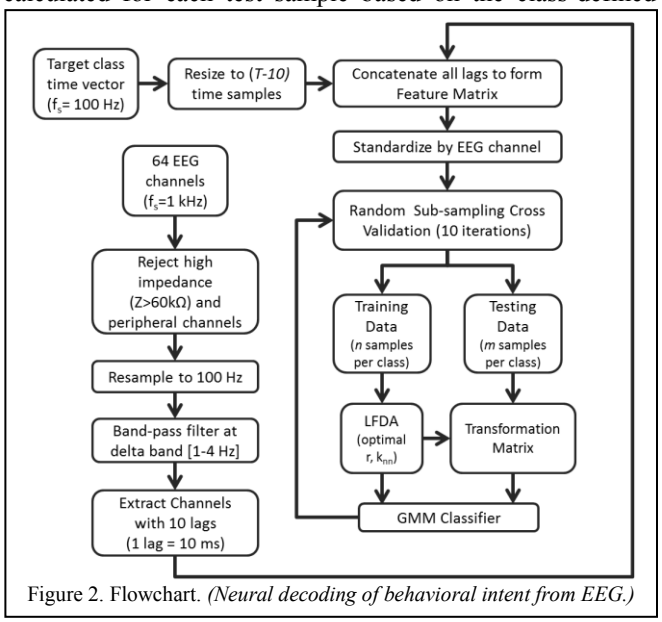

Figure 2. Flowchart. *(Neural decoding of behavioral intent from EEG.)*

III. Results

A. Motion Artifact Analysis

Due to the unconstrained nature of the infant's actions, we analyzed and compared the frequency content of both EEG and acceleration data from the IMUs to observe any spectral relationships between EEG and acceleration. Since any movement-related artifacts would most likely originate from head movement, only acceleration information from the head sensor was acquired for further analysis in this paper.

We computed the coherence, or relationship between two signals within the frequency domain, in a manner similar to the short-time Fourier transform in order to generate the coherence spectrogram plot displayed in Fig. 3. High coherence values indicate a strong relationship between the two analyzed signals, as is the case between the head acceleration and each corresponding EEG electrode within the 0.1 – 1 Hz range. Since this strong relationship may be a result of low frequency artifacts, only frequencies between 1 – 4 Hz (higher in the delta frequency sub-band) were band-pass filtered for further neural decoding analyses.

B. Infant Task Classification

Decoding resulted in an overall mean accuracy of 80.50 ± 1.03%, which was well above the chance level of 16.67%. Ten iterations of the random sub-sampling cross validation procedure (Fig. 2) were performed to provide the mean classification accuracies. By observing the percentage of (mis) classified samples relative to each training set size per class, a training set-normalized confusion matrix was generated as shown in Fig. 4 where each block contains a percentage of training set samples either classified or misclassified to its respective class. We note high percentages along the diagonal of this matrix indicating a high degree of accurate classification for each class. Misclassification was more apparent for 'explore' (0.8-21.1%), 'reach-grasp' (1.7-14.3%), and 'attentive rest' (0-8.2%), unlike the low misclassifications of 'point' (0%) and 'imitate' (0-0.1%) actions.

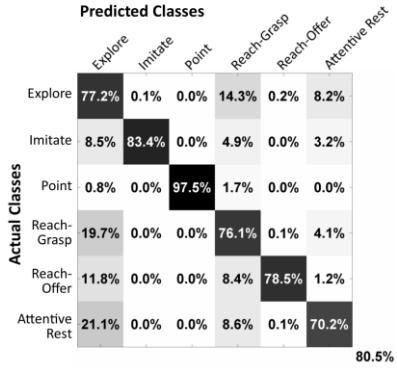

Figure 4. Training Set-Normalized Confusion Matrix. *(Overall mean accuracy of 80.50 ± 1.03%. Percentages reflect the ratio between the number of samples classified and the number of testing samples per class. Adjustable LFDA parameters were optimized to r {number of reduced dimensions} = 200 and k_{nn} {number of k-nearest neighbors} = 11.*

The most informative channels were revealed by applying a forward selection method [15] to each channel and were located primarily in motor and premotor areas, specifically channels FC6, FC3, C1, FC4, and F5.

IV. Discussion

Our results demonstrate the feasibility of decoding goal-oriented (intentional) behavioral actions from scalp EEG in freely behaving infants. These results show that scalp EEG contain valuable predictive information about the infant's intent. Though only a case study, our results already start to provide insights on how goal-oriented actions may be represented in brain activity as measured with scalp EEG. Further, goal-directed tasks such as *point* and *imitate* yielded higher classification accuracies than tasks without a clear end goal such as explore and rest. Thus, tasks such as *imitate* or *point* may have simply performed better because the infant presented a clear and direct objective/goal in his or her mind, whereas the confusion in classifying *explore* and *attentive rest* tasks may be indicative of the infant's attempts to understand the environment or the intent of the experimenter. In summary, the proposed novel methodology provides a window to study the neural activity underlying mirror neuron system (goal-oriented) tasks in freely behaving infants. It also suggests an alternative to the μ-rhythm account of MNS function by providing a predictive, network-based account of intentionality in freely behaving infants based on scalp EEG.

References

[1] Gallese V, Fadiga L, Fogassi L, Rizzolatti G. (1996). Action recognition in the premotor cortex. *Brain* 9 (Pt 2): 593-609.

[2] Cuevas K, Cannon EN, Yoo K, Fox NA. (2014). The infant EEG mu rhythm: methodological considerations and best practices. *Dev Rev.* 34 (1): 26-43. doi: 10.1016/j.dr.2013.12.001

[3] Southgate V, Johnson MH, Osborne T, Csibra G. (2009). Predictive motor activation during action observation in human infants. *Biol Lett.* 5(6): 769–772.

[4] Woodward AL, Guajardo JJ. (2002). Infants' understanding of the point gesture as an object-directed action. *Cogn Dev.* 17: 1061-1084.

[5] Vanderwert RE, Fox NA, Ferrari PF (2013). The mirror mechanism and mu rhythm in social development. *Neurosci Lett.* 540: 15-20. doi: 10.1016/j.neulet.2012.10.006

[6] Hickok G. (2009). Eight problems for the mirror neuron theory of action understanding in monkeys and humans. *J Cogn Neurosci.* 2009 Jul, 21(7): 1229-43. doi: 10.1162/jocn.2009.21189

[7] Hochberg LR, Bacher D, Jarosiewicz B, Masse NY, Simeral JD, Vogel J, Haddadin S, Liu J, Cash SS, van der Smagt P, Donoghue JP. (2012). Reach and grasp by people with tetraplegia using a neurally controlled robotic arm. *Nature* 485: 372–5.

[8] Hernandez ZR, Cruz-Garza JG, Nepaul S, Bradley KK and Contreras-Vidal JL (2014). Neural decoding of expressive human movement from scalp electroencephalography (EEG). *Front. Hum. Neurosci.* 8 (188). doi: 10.3389/fnhum.2014.00188

[9] Becchio C, Sartori L, Bulgheroni M, Castiello U. (2008). The case of Dr. Jekyll and Mr. Hyde: A kinematic study on social intention. *Conscious Cogn.* 17 (3): 557-564.

[10] Cannon EN, Yoo KH, Vanderwert RE, Ferrari PF, Woodward AL, et al. (2014). Action Experience, More than Observation, Influences Mu Rhythm Desynchronization. *PLoS ONE* 9(3): e92002. doi:10.1371/journal.pone.0092002

[11] Claxton, Laura J., Rachel Keen, and Michael E. McCarty. (2003). "Evidence of motor planning in infant reaching behavior." *Psychol Sci.* 14(4): 354-356.

[12] Marins JL, Yun X, Bachmann ER, McGhee RB, and Zyda MJ. (2001). "An extended Kalman filter for quaternion-based orientation estimation using MARG sensors," in *Conf Proc IEEE/RSJ Intell Robot Syst.* Vol. 4, 2003–2011. doi: 10.1109/IROS.2001.976367

[13] Li W, Prasad S, Fowler JE, and Bruce LM. (2012). Locality-preserving dimensionality reduction and classification for hyperspectral image analysis. *IEEE T Geosci Remote.* 50, 1185–1198. doi: 10.1109/TGRS.2011.2165957

[14] Sugiyama, M. (2006). "Local Fisher discriminant analysis for supervised dimensionality reduction," in *Proc 23rd ICML.* 905–912. doi: 10.1145/1143844.1143958

[15] Pagano M, and Gauvreau, K. (2000). "Multiple Regression," in *Principles of bio-statistics,* 2nd Ed., eds C. Crockett, et al. (Pacific Grove, CA: Duxbury), 449–469.

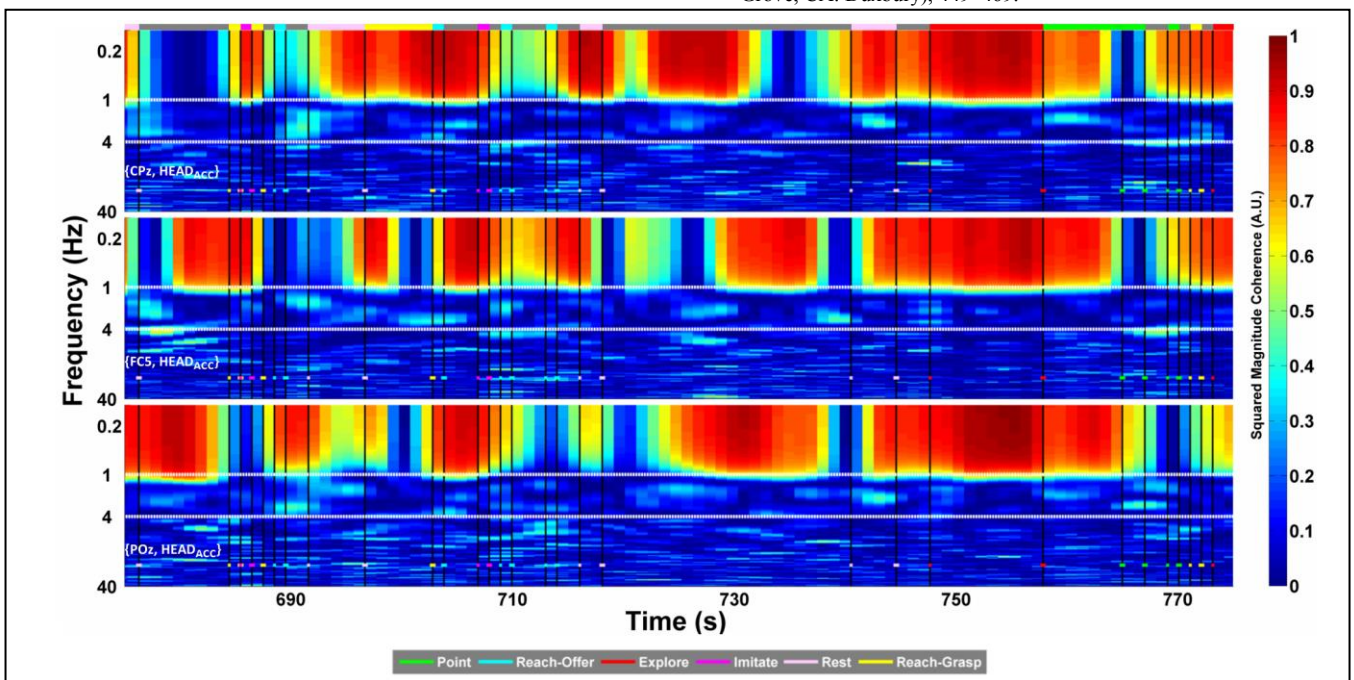

Figure 3. Coherence Spectrogram. *Coherence values indicate the relationship between EEG channels and head IMU acceleration. High coherence is noticeable within the 0.1 – 1 Hz range. Dotted white lines indicate the band-pass frequency cutoffs(1 – 4 Hz) to avoid contamination of motion-related artifacts. The plot represents a subset of acquired data but all actions showed the same pattern of coherence.*